First-contact time to a patch in a multidimensional potential well

Le Yang,[1] David Sept,[1,2,3] and A. E. Carlsson[1,3]
[1]*Department of Physics, Washington University, St. Louis, Missouri 63130, USA*
[2]*Department of Biomedical Engineering, Washington University, St. Louis, Missouri 63130, USA*
[3]*Center for Computational Biology, Washington University, St. Louis, Missouri 63130, USA*
(Received 4 May 2007; revised manuscript received 25 June 2007; published 9 August 2007)

The escape of a diffusing particle from a potential well is an important aspect of many dynamic processes in chemistry, physics, and biology, and such an escape process often involves finding a restricted region or patch in a multidimensional potential well. We study an idealized model of this process via simulation and analytic theory. By combining results from special cases having either high symmetry or zero potential, we obtain a simple formula for the first-contact time for a particle moving to a boundary patch in an arbitrary number of dimensions. We apply this formula in two, three, and six dimensions. The predicted dependences of the first-contact time on the well depth and patch size are compared to results from simulations, and close agreement is found. We extend the theory to calculate the first-contact time between two particles in separate harmonic potential wells. As an application of this extended theory, we calculate the first-contact time for two parallel semiflexible biopolymer filaments and compare these results to previous simulations.

DOI: 10.1103/PhysRevE.76.021911 PACS number(s): 82.39.−k, 87.16.−b, 02.50.−r, 05.40.−a

I. INTRODUCTION

The problem of the escape of a particle from a classical potential well is related to numerous dynamic phenomena in physics, chemistry, and biology [1,2]. Several theories of escape have been developed, including transition-state theory [3–5], Kramers rate theory [6,7], unimolecular rate theory [8–10], and the mean-first-passage-time approach [11,12]. The one-dimensional case is the best understood, and many dynamic problems can be reduced to that of a particle moving between two metastable states, separated by a one-dimensional potential barrier. According to transition-state theory, the escape time (or the first-contact time for the particle to reach the top of the potential barrier) for large barrier heights E_0 is generally proportional to $\exp(\beta E_0)$, where $\beta = 1/k_B T$. The time predicted by this theory is always larger than the actual time [1]. In Kramers theory, the escape time from a harmonic potential well is proportional to $\exp(\beta E_0)/(\beta E_0)$ for a potential with a smoothed boundary [7]. Mean-first-passage-time theory [1] gives the same result for this case, but gives an answer proportional to $\exp(\beta E_0)/(\beta E_0)^{3/2}$ for a cusp-shaped barrier. For the escape of a particle from a spherical N-dimensional harmonic potential well with a cusp-shaped boundary, a recent study by Zhu and Carlsson [13] demonstrated via mean-first-passage-time theory that the first-contact time is proportional to $\exp(\beta E_0)/(\beta E_0)^{N/2+1}$.

In higher-dimensional problems, one often seeks to determine the first-contact time of a particle to a "patch" or a small portion of a constant-energy surface. This problem has reduced symmetry and, to our knowledge, has not been treated analytically in the presence of a potential. However, some intuition can be gained by studying the simpler problem of the first-contact time for a free particle moving from an outer reflecting boundary to a smaller absorbing boundary, which is taken to be the patch. The equation determining the first-contact time W is $\nabla^2 W + 1/D = 0$ [14], where D is the diffusion constant of the particle. Application of this equation to the simplified problem of circular boundaries in two dimensions yields $W(b) = (2b^2 \ln b/s - b^2 + s^2)/4D$, where b is the radius of the reflecting boundary and s is the radius of the absorbing boundary [15]. Analogous results hold for higher dimensions. The first-contact time calculated in this way is not inversely proportional, as one might expect from a ballistic treatment, to the boundary area of the patch. In the two-dimensional case considered here, W scales logarithmically with s for small s. In three dimensions, $W \propto 1/s$. This departure from ballistic behavior occurs because free diffusion is a volume-filling process [16].

In this paper, we use a combination of Brownian dynamics simulations and analytic theory to develop a simple formula for the first-contact time of a particle to a patch in a multidimensional potential well. The Brownian dynamics simulations treat a particle moving in a harmonic potential well, with boundary conditions determined by the patch, using a Green's function method. The analytic theory treats the first-contact time of a free particle to a patch in two, three, and six dimensions. We build on this result and the previous results for spherical symmetry [13], to obtain a formula for the first-contact time to a patch in a harmonic potential well. We evaluate the accuracy of this formula by comparison with the Brownian dynamics simulations.

We then extend our theory to calculate the first-contact time between two moving particles, each of which is in its own harmonic potential well. This extension allows us to calculate the first-contact time between two constrained, parallel, semiflexible biopolymer filaments. The first-contact time is important since it is equivalent to the bundling time for strong attractive interfilament interactions. Previously, we have used simulations based on a normal-mode approach to describe the motion of semiflexible filaments [17]. In this approach, the time dependence of each normal-mode coefficient is identical to that of a particle in a harmonic potential well. The motion of each part of a filament can be reduced that of the lowest normal mode, provided the filament is given a larger effective contact radius to account for the ef-

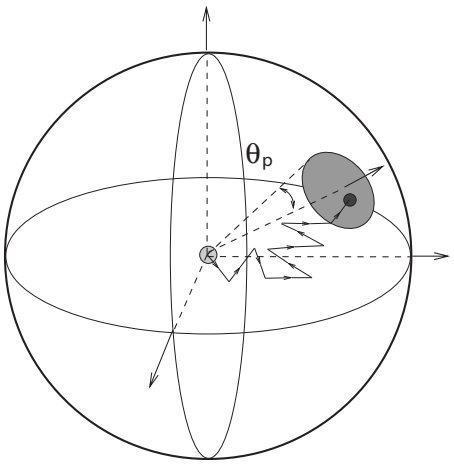

FIG. 1. Schematic of the first-contact time for a particle to a patch in three-dimensional space. The patch size is θ_p.

fects of the higher modes. The earlier simulations showed that most contact occurs between the tips of filaments. Thus we are justified in approximating the motions of the filaments by the motions of particles, and we can employ the formulas developed here to predict the first-contact time between the filaments.

II. SIMULATION METHODS

A. Model

The first-contact time problem for a particle to a patch on a sphere in three-dimensional space is shown in Fig. 1. The patch indicated in gray, which has absorbing boundary conditions, is a cap on the boundary of the sphere. The rest of the sphere has reflecting boundary conditions. The angular size of the patch is θ_p. The particle starts moving from the center of the sphere, which coincides with the bottom of the potential well, and will typically be reflected many times by the reflecting part of the boundary before it finally contacts the absorbing patch. The first-contact time is the time to reach the absorbing patch. To simplify the calculation, we let the center of the patch be $(R,0,0)$ in spherical coordinates. Then the patch is defined by $(r=R, 0 \le \phi < 2\pi, 0 \le \theta < \theta_p)$ in three-dimensional space.

Generally, the patch in N-dimensional space can be described as

$$r = R, \quad \phi \in [0,2\pi], \quad \theta_1 \in [0,\pi], \ldots,$$
$$\theta_{N-3} \in [0,\pi], \ldots, \theta_{N-2} \in [0,\theta_p],$$

where $\phi, \theta_1, \ldots,$ and θ_{N-2} are the angular variables in N-dimensional spherical coordinates. We use a harmonic potential $E(r)=k|\vec{r}|^2/2$, where k is a spring constant and $\vec{r}$ is the position vector of the particle. In addition to letting the particle start at the center of the sphere, we have also let the initial position be randomly distributed throughout the sphere with probability $P(\vec{r}) \propto \exp[-\beta E(\vec{r})]$, and found little change in the results. The simulations show that the dependence of the first-contact time on initial position is very weak, provided that the potential on the boundary is much larger than k_BT.

B. Brownian dynamics

To simulate the Brownian motion of a particle in the harmonic potential well, we use a Green's function method as detailed in our previous work [17]. The Green's function gives the probability density that the position of the particle is $\vec{r}$ at time $t+\Delta t$, given that it was at $\vec{r}'$ at time t. The Green's function for a harmonic potential well [18] is

$$G(\vec{r},\vec{r}';\Delta t) = [2\pi B(\Delta t)]^{-N/2} \exp\left(-\frac{|\vec{r}-\vec{A}(\Delta t)|^2}{2B(\Delta t)}\right),$$

where

$$\vec{A}(\Delta t) = \vec{r}' \exp(-\Delta t/\tau),$$

$$B(\Delta t) = k_B T[1-\exp(-2\Delta t/\tau)]/k,$$

and

$$\tau = \frac{k_B T}{Dk}.$$

Here D is the diffusion constant of the particle, and τ is its relaxation time.

From this Green's function, we calculate the updated value of the position of the particle at each time step as

$$\vec{r}(t+\Delta t) = \vec{A}(\Delta t) + B(\Delta t)\vec{\sigma},$$

where each component of the N-dimensional vector $\vec{\sigma}$ has a normal distribution with a variance of unity.

We choose the time step Δt as follows. For most cases, the upper bound is $1.5\times10^{-3}R^2/D$, which gives a typical displacement much smaller than R. Near the boundary, a smaller time step is needed to avoid spurious boundary crossings, so we use $\Delta t=0.01(R-r)^2/2D$ for those values of r where this is less than the previous bound. However, we impose a lower bound of $1.5\times10^{-6}R^2/D$, which is needed to allow the particle to escape. This gives a displacement of about $2\times10^{-3}R$ per time step, which is much less than our patch sizes. We regard the particle as contacting the patch if the particle is outside the boundary and within the angular range of the patch. We note that there is no required criterion of small energy or force change during a time step, because the Green's function treats the force exactly. We statistically average over 100 runs.

III. ANALYTIC TREATMENT OF SPECIAL CASES

As background for our derivation, we first present and evaluate the analytic forms for two simpler but related problems: a particle moving to a boundary with spherical symmetry, and a particle moving to a patch with no potential. The first-contact time W in the presence of a potential can be obtained by solving

$$\nabla^2 W - \beta \nabla E \cdot \nabla W + \frac{1}{D} = 0, \tag{1}$$

with proper boundary conditions [19]: $W=0$ on the absorbing part of the boundary, and its normal derivative $\partial W/\partial r=0$ on the reflecting part.

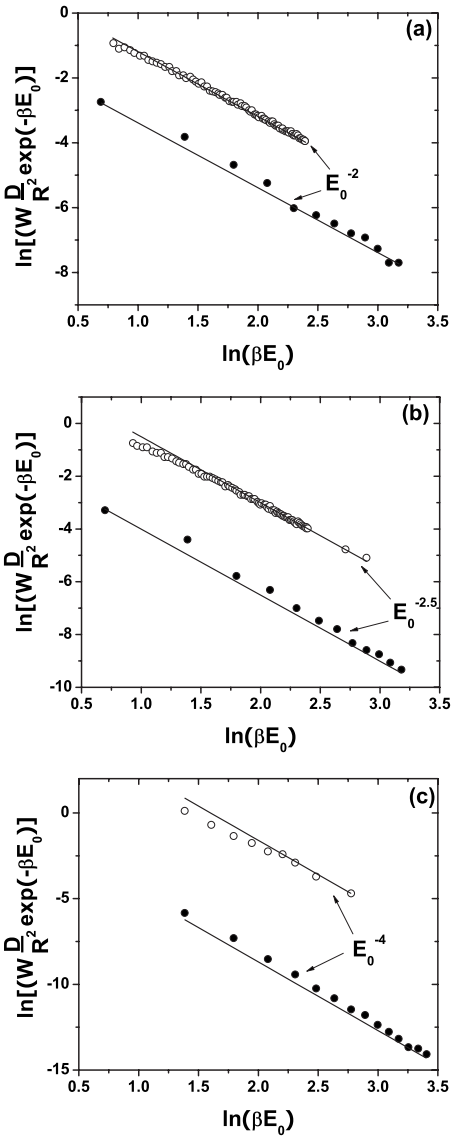

FIG. 2. Calculations and simulations of the first-contact time for a particle in a potential well to the entire boundary (filled circles and accompanying lines) and patch (open circles and accompanying lines) as functions of potential in (a) two-, (b) three-, and (c) six-dimensional space. The patch size is fixed, $\theta_p=0.35$.

A. Particle in harmonic potential well to boundary in N dimensions

In this case, the patch becomes the entire boundary and the symmetry is spherical. W is obtained in N-dimensional space by solving Eq. (1) with entirely absorbing boundary conditions. As mentioned above, the result for large E_0 is [13]

$$W(0) = C_N \frac{R^2}{2ND} \frac{e^{\beta E_0}}{(\beta E_0)^{N/2+1}}, \tag{2}$$

where $E_0=kR^2/2$ is the potential on the boundary and the C_N are constants depending on N; $C_1=\sqrt{\pi}/2$, $C_2=1$, $C_3=3\sqrt{\pi}/4$, $C_4=2$, $C_5=15\sqrt{\pi}/8$, and $C_6=6$. The filled dots and the accompanying line in Fig. 2 compare the simulations and calculations of the particle in a harmonic potential well to the boundary in two, three, and six dimensions. We see that Eq. (2) agrees with the simulation results to within 50% over several orders of magnitude variation in W. The agreement between the theory and the simulations is not perfect because the theory is exact only in the limit of very deep potentials; it is seen in the figure that the agreement improves with increasing potential depth.

B. Calculation of first-contact time for a free particle to a patch

We solve the first-contact equation Eq. (1) by writing its solution as the sum of a solution of the inhomogeneous equation, which does not satisfy the boundary conditions, and a correction term δW, which satisfies the corresponding homogeneous equation and corrects the boundary conditions. If we define $W=-r^2/2ND+\delta W$, the symmetry of the problem implies that δW is a function of only r and θ_{N-2}, which is abbreviated as $\theta=\theta_{N-2}$ to simplify the notation, and the first-contact-time equation implies that

$$\nabla^2 \delta W(r,\theta) = 0 \tag{3}$$

with boundary conditions

$$\delta W(R, \theta < \theta_p) = \frac{R^2}{2ND},$$

$$\frac{\partial \delta W}{\partial r}(R, \theta > \theta_p) = \frac{R}{ND}.$$

We notice that, from Gauss's law,

$$\int_S \frac{\partial}{\partial r} \delta W \, ds = \int_V \nabla^2 \delta W \, dV = 0.$$

To obtain an approximate result, we assume that $\frac{\partial \delta W}{\partial r}$ takes on constant values inside both the reflecting and absorbing boundaries. Then, from the above equation, we have

$$s_N^{\text{patch}} \frac{\partial}{\partial r} \delta W(R, \theta < \theta_p) + (s_N - s_N^{\text{patch}}) \frac{\partial}{\partial r} \delta W(R, \theta \geq \theta_p) = 0,$$

where s_N^{patch} is the area of the patch, and s_N is the area of the entire boundary in N dimensions. So the boundary condition at $r=R$ is

$$\frac{\partial \delta W}{\partial r} = \begin{cases} \dfrac{R}{ND}, & \theta > \theta_p, \\ -\dfrac{R}{ND} \dfrac{(s_N - s_N^{\text{patch}})}{s_N^{\text{patch}}}, & \theta < \theta_p. \end{cases}$$

In two dimensions, the area of the patch is $s_{N=2}^{\text{patch}}=2R\theta_p$, and $s_{N=2}=2\pi R$. In three dimensions, $s_{N=3}^{\text{patch}}=2\pi R^2(1-\cos\theta_p)$, which becomes $\pi R^2\theta_p^2$ for small θ_p, while $s_{N=3}=4\pi R^2$. In order to evaluate the validity of our model for higher-dimensional escape processes, we also consider the case $N=6$. Here $s_{N=6}=\pi^3 R^5$, and we find $s_{N=6}^{\text{patch}}=\pi^2 R^5[\theta_p-(2/3)\sin(2\theta_p)+(1/12)\sin(4\theta_p)]$, which becomes $s_{N=6}^{\text{patch}} \approx (8/15)\pi^2 R^5 \theta_p^5$ if θ_p is small.

In three dimensions, it is well known that a solution of Eq. (3) that is regular at the origin can be written as a sum of terms proportional to $r^l P_l(\cos\theta)$, where the P_l are the Legendre polynomials and $l \geq 0$. The generalizations of the Legendre polynomials to N dimensions are the Gegenbauer polynomials $C_l^{(m)}(\cos\theta)$, where $m=N/2-1$. Thus we write

$$\delta W = \sum_{l=0}^{\infty} A_l C_l^{(N/2-1)}(\cos\theta) r^l.$$

Then at $r=R$,

$$\frac{\partial \delta W}{\partial r} = \sum_{l=1}^{\infty} l A_l C_l^{(N/2-1)}(\cos\theta) R^{l-1}. \tag{4}$$

On the other hand, the boundary condition on $\frac{\partial \delta W}{\partial r}$ prescribed at R can be expanded as follows in the Gegenbauer polynomials:

$$\frac{\partial \delta W(R,\theta)}{\partial r} = \sum_l a_l C_l^{(N/1-2)}(x), \tag{5}$$

where $x=\cos\theta$, and the coefficients have different forms for $N=2$,

$$a_l = \frac{l^2}{2\pi}\int_{-1}^{1} C_l^{(0)}(x)(1-x^2)^{-1/2}\frac{\partial \delta W(R,\theta)}{\partial r}dx,$$

and for $N>2$,

$$a_l = \frac{l!\,(l+N/2-1)\Gamma(N/2-1)^2}{\pi 2^{3-N}\Gamma(l+N-2)}\int_{-1}^{1} C_l^{(N/2-1)} \times (1-x^2)^{(N-3)/2}\frac{\partial \delta W(R,\theta)}{\partial r}dx.$$

Comparing Eqs. (4) and (5), we have

$$A_l = \frac{a_l}{l R^{l-1}}, \quad l \geq 1.$$

So

$$W(0,0) = W(0,0) - W(R,0) = R^2/2ND - R\sum_{l=1}^{\infty}\frac{a_l}{l}C_l^{(N/2-1)}(1),$$

where the first equality holds since by assumption $W(R,0)=0$. At $x=1$, the Gegenbauer polynomials have the values $C_l^{(0)}(1)=2/l$ for $N=2$, $l\neq 0$, and $C_l^{(N/2-1)}(1)=(l+N-3)!/[l!(N-3)!]$ for $N>2$. Therefore, for $N=2$,

$$W(0,0) = \frac{R^2}{4D} - \frac{R}{\pi}\sum_{l=1}^{\infty}\int_{-1}^{1} C_l^{(0)}(x)(1-x^2)^{-1/2}\frac{\partial \delta W(R,\theta)}{\partial r}dx, \tag{6}$$

and for $N>2$,

$$W(0,0) = R^2/2ND - \frac{R}{\pi}\frac{\Gamma(N/2-1)^2}{2^{3-N}(N-3)!}\sum_{l=1}^{\infty}[1+(N/2-1)/l] \times \int_{-1}^{1} C_l^{(N/2-1)}(x)(1-x^2)^{(N-3)/2}\frac{\partial \delta W(R,\theta)}{\partial r}dx. \tag{7}$$

In evaluating these sums, we note that, in each of the integrals, any constant can be added to the integrand without changing the result, since $C_l^{(N/2-1)}$ for $l>1$ is orthogonal (with respect to the weighting function in the integrals) to $C_0^{(N/2-1)}$, which is a constant. Therefore, adding $-R/ND$ to the integrand, we obtain

$$\int_{-1}^{1} C_l^{(N/2-1)}(x)(1-x^2)^{(N-3)/2}\frac{\partial \delta W}{\partial r}dx = -\frac{R s_N}{ND s_N^{\text{patch}}}\int_{x_p}^{1} C_l^{(N/2-1)}(x)(1-x^2)^{(N-3)/2}dx,$$

where $x_p=\cos\theta_p$. Furthermore, the sums over l can be evaluated using the generating function [20] for the Gegenbauer polynomials:

$$\sum_{l=0}^{\infty} C_l^0(x)t^l = -\ln(1-2xt+t^2) \quad (N=2), \tag{8}$$

$$\sum_{l=0}^{\infty} C_l^{N/2-1}(x)t^l = \frac{1}{(1-2xt+t^2)^{N/2-1}} \quad (N>2), \tag{9}$$

which, using the fact that $C_0^{N/2-1}(x)=1$, gives

$$\sum_{l=1}^{\infty} C_l^0(x) = -\ln(2-2x) - 1 \quad (N=2), \tag{10}$$

$$\sum_{l=1}^{\infty} C_l^{N/2-1}(x) = \frac{1}{(2-2x)^{N/2-1}} - 1 \quad (N>2). \tag{11}$$

For $N>2$, there is also a sum in Eq. (7) of the form

$$\sum_{l=1}^{\infty} C_l^{N/2-1}(x)/l. \tag{12}$$

This sum is less divergent when $x\to 1$ than $\Sigma_{l=0}^{\infty} C_l^{N/2-1}(x)$. To see this, we divide Eq. (9) by t to obtain $\Sigma_{l=0}^{\infty} C_l^{N/2-1}(x)t^{l-1} = 1/[t(1-2xt+t^2)^{N/2-1}]$. Moving the $l=0$ term to the right-hand side, using the fact that $C_0^{N/2-1}(x)=1$, and integrating both sides from 0 to t, we have

$$\sum_{l=1}^{\infty} C_l^{N/2-1}(x)t^l/l = \int_0^t dt[(1-2xt+t^2)^{1-N/2}-1]/t. \tag{13}$$

We seek the behavior of this integral for x near 1, in the limit that $t\to 1$. The part of the integral between 0 and 1/2 (chosen arbitrarily) approaches a constant value as $x\to 1$, so we ignore it in the following since it is dominated by the singular parts. Similarly, in the part between 1/2 and 1 we can ignore the last -1 term since its contribution also approaches a constant. We establish the asymptotic behavior of

Eq. (13) by placing upper and lower bounds on it. To establish the upper bound, we write the integrand as $[(1-t)^2+2t(1-x)]^{1-N/2}/t$. An upper bound on this is obtained by replacing the second and third t's by 1/2. This gives an upper bound on the singular part of the integral, of $2\int_0^t dt[(1-t)^2+(1-x)]^{1-N/2}$. By the straightforward change of variables $u=(1-t)/(1-x)^{N/2-1}$, one readily shows that for x near 1, the asymptotic behavior is proportional to $(1-x)^{3/2-N/2}$. A similar proportionality (but with a different prefactor) is obtained for the lower bound, by substituting $t=1$ instead of $t=1/2$. Thus, for x near 1, Eq. (12) is proportional to $(1-x)^{3/2-N/2}$, which is less singular than Eq. (11), and can be ignored.

Therefore, combining Eqs. (6), (7), (10), and (11), we have for $N=2$,

$$W(0,0) = \frac{R^2}{4D} + \frac{R^2 s_N}{2\pi D s_N^{\text{patch}}} \int_{x_p}^{1} [-\ln(2-2x)-1](1-x^2)^{-1/2} dx, \tag{14}$$

and for $N>2$,

$$W(0,0) = \frac{R^2}{2ND} + \frac{R^2 s_N}{\pi N D s_N^{\text{patch}}} \frac{\Gamma(N/2-1)^2}{(N-3)!\,2^{3-N}} \times \int_{x_p}^{1} \frac{1}{(2-2x)^{N/2-1}} (1-x^2)^{(N-3)/2} dx, \tag{15}$$

where we have assumed θ_p to be small and kept only the most singular terms in the $N>2$ case.

Evaluating Eq. (14) using the substitution $x=\cos\theta$, and using the approximation $\cos\theta \simeq 1-\theta^2/2$, we obtain for two dimensions

$$W(0,0) = \frac{R^2}{4D}(3 - 4\ln\theta_p). \tag{16}$$

For $N>2$, evaluating Eq. (15) for x_p close to 1, we obtain

$$W(0,0) = \frac{R^2}{2ND} + \frac{R^2 s_N}{\pi N D s_N^{\text{patch}}} \frac{\Gamma(N/2-1)^2}{(N-3)!\,2^{3-N}} \theta_p. \tag{17}$$

Thus, for $N=3$,

$$W(0,0) = \frac{R^2}{6D} + \frac{4R^2}{3D\theta_p}, \tag{18}$$

and for $N=6$,

$$W(0,0) = \frac{R^2}{12D} + \frac{5R^2}{12D\theta_p^4}, \tag{19}$$

Figure 3 shows the very good agreement obtained between the simulations and the analytic theory for a free particle contacting a patch in two, three, and six dimensions.

IV. PARTICLE IN POTENTIAL WELL TO PATCH

To obtain the first-contact time for a particle in a potential well to a patch, one would need to solve Eq. (1) with the mixed boundary conditions. We see no analytical way of doing this, so we focus instead on developing an approximate formula for the first-contact time, valid over a limited range of conditions. We saw above that the first-contact time for a free particle to a patch is not proportional to the boundary area of the patch. This occurs because the particle remains in the general vicinity of the patch for a long enough time that it can make numerous attempts to escape. This weakens the dependence of W on the patch size. However, in the presence of a strong restoring potential pulling the particle away from the general vicinity of the patch (or indeed the entire boundary), the particle spends a shorter time in the vicinity of the patch. Thus we expect a stronger dependence on patch size. Our simulations confirm these expectations, and show that for strong potentials, the path leading to escape is often a nearly straight line from the potential's center

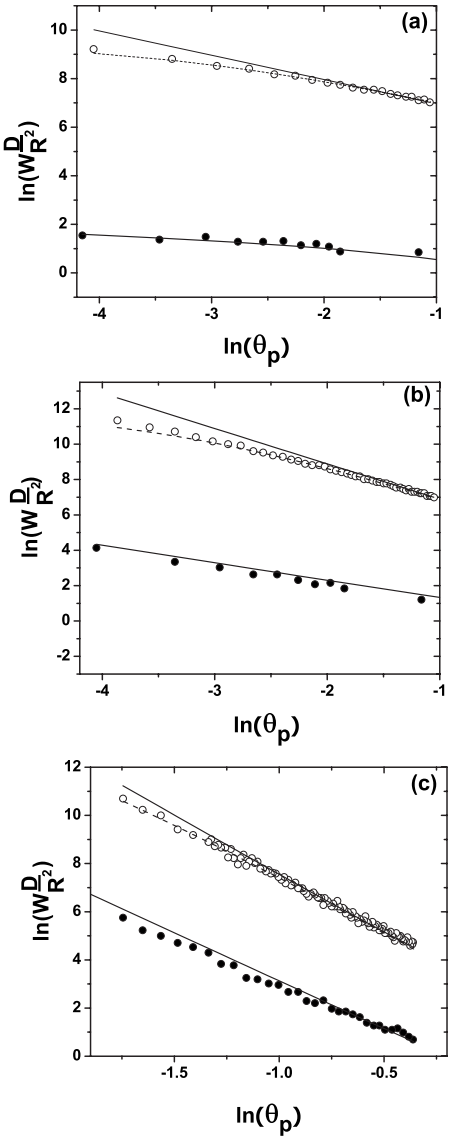

FIG. 3. Calculations and simulations of the first-contact time for a particle in a potential well (open circles and accompanying lines) and free particle (filled circles and accompanying lines) moving to a patch, as a function of patch size in (a) two-, (b) three-, and (c) six-dimensional space. The potential is fixed, $E_0=11k_BT$. Solid lines: calculations using Eqs. (20) and (22). Dashed lines: calculations using Eq. (24).

to the patch. Therefore, a plausible assumption is that the first-contact time is inversely proportional to the area, and this is confirmed by our simulations described below.

The qualitative difference between the behavior for zero potential and that for strong potentials suggests a transition occurring as a function of well depth. This transition may be understood by considering a population of particles in the well of density $c(\vec{r})$, in equilibrium except for the region near the patch where the outward current is appreciable. The inverse of the first-contact time, or the escape rate, is then proportional to the current I of particles going through the patch, which in turn is proportional to $|\vec{\nabla}c|s_N^{\text{patch}}$; s_N^{patch} is proportional to θ_p^{N-1} for small θ_p. If the well depth is small, $\vec{\nabla}c$ around the patch results mainly from the θ dependence of the boundary condition. Therefore we expect that $\vec{\nabla}c \propto c/\theta_p R$, where $\theta_p R$ is the linear size of the patch, so that $I \propto \theta_p^{N-1}/\theta_p = \theta_p^{N-2}$. If the potential is very strong, then $\vec{\nabla}c$ is dominated by the effects of the potential. One readily shows that this gives $|\vec{\nabla}c| \approx c2\beta E_0/R$, which is independent of θ_p. Thus, in this limit, $I \propto \theta_p^{N-1}$. The transition between the two regimes will occur at $\theta_p \approx 1/(2\beta E_0)$.

Therefore, in extending Eq. (2) to treat motion to a patch, we use a stronger dependence on θ_p than for the free-particle case. We hypothesize the following separable form for the first contact time for large E_0:

$$W_N = C_N \frac{R^2}{2ND} \frac{s_N}{s_N^{\text{patch}}} \frac{e^{\beta E_0}}{(\beta E_0)^{N/2+1}},$$

where the energy dependence is taken from Eq. (2). In the limit of the patch being the entire boundary, this result reproduces Eq. (2). In two, three, and six dimensions, we obtain

$$W_2 = \frac{R^2}{4D} \frac{\pi}{\theta_p} \frac{e^{\beta E_0}}{(\beta E_0)^2}, \tag{20}$$

$$W_3 = \frac{\sqrt{\pi} R^2}{8D} \frac{2}{1-\cos\,\theta_p} \frac{e^{\beta E_0}}{(\beta E_0)^{5/2}}, \tag{21}$$

$$W_6 = \frac{R^2}{2D} \frac{\pi}{\theta_p - \frac{2}{3}\sin(2\theta_p) + \frac{1}{12}\sin(4\theta_p)} \frac{e^{\beta E_0}}{(\beta E_0)^4}. \tag{22}$$

If the patch is small, we can expand the area of the patch as a function of θ_p and obtain a general formula for the first-contact time of a particle in a potential well to a small patch:

$$W_N = C_N' \frac{R^2}{2ND} \frac{e^{\beta E_0}}{(\beta E_0)^{N/2+1}} \frac{1}{\theta_p^{N-1}}, \tag{23}$$

where $C_2' = \pi$, $C_3' = 3\sqrt{\pi}$, and $C_6' = 45\pi/4$.

Figure 2 (open circles) shows the simulations and calculations of the first-contact time of a particle in a harmonic potential well to a patch as a function of the potential depth E_0. We again see that the agreement of the analytic theory of Eqs. (20) and (22) with the simulations is within a factor of 2, over two orders of magnitude variation in W. The log-log plot is a straight line, with a slope identical to the case of a completely absorbing boundary. Figure 3 shows the first-contact time as a function of the patch size θ_p. As expected

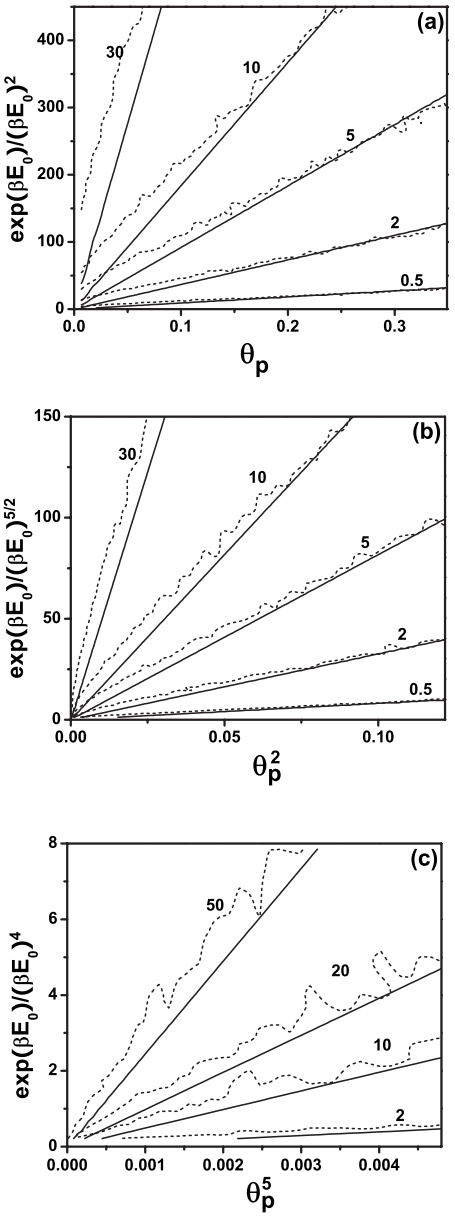

FIG. 4. Contour plot of analytic theory (solid lines) and simulations (dashed lines) of the first contact time for a particle in a potential well to a patch as a function of potential and patch size in (a) two-, (b) three-, and (c) six-dimensional space. Numbers on contour lines give first-contact time in seconds. Solid lines are calculated using Eq. (23).

from the discussion above, we see that the slopes in the log-log plot of the first-contact time are different from those for a free particle. Equations (20) and (22) are close to the simulations for moderately small patch sizes, but for very small patch sizes the dependence on θ_p becomes weaker, as expected from our analysis. The transition as a function of θ_p occurs at $\theta_p \approx 1/(\beta E_0)$, roughly consistent with the above expectations.

The global accordance of Eq. (23) with the simulation results is shown in Fig. 4, which is a contour plot as a function of $e^{\beta E_0}/(\beta E_0)^{N/2+1}$ and θ_p^{N-1}. Since Eq. (23) is separable, the corresponding contour lines are straight. The simulation

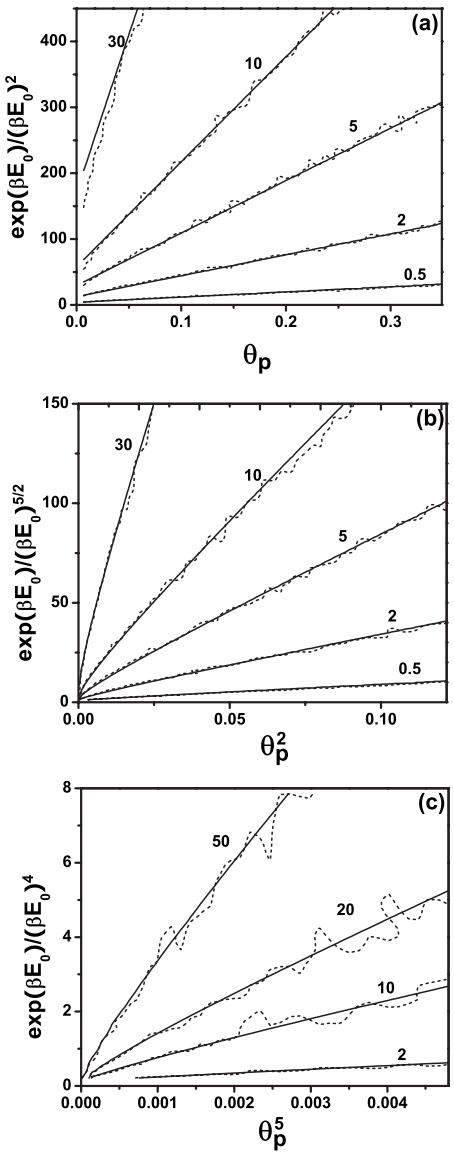

FIG. 5. Contour plot of the corrected calculations (solid lines) and simulations (dashed lines) of the first-contact time for a particle in a potential well to a patch as a function of potential and patch size in (a) two-, (b) three-, and (c) six-dimensional space. Numbers on contour lines give first-contact time in seconds. The solid lines are calculated using Eq. (24).

lines are almost straight, and the calculations are fairly close to the simulations. However, there is a relative shift of the simulations relative to the calculations around the origin. To obtain a better estimate of W, we put additional parameters (p_1, p_2, p_3) into the formula,

$$W_N = p_1 C'_N \frac{R^2}{2ND}\left(\frac{e^{\beta E_0}}{(\beta E_0)^{N/2+1}} + p_2\right)\left(\frac{1}{\theta_p + p_3}\right)^{N-1}. \quad (24)$$

By fitting to the simulations, we obtain the following parameter values: $p_1 = 1.15, 1.17, 1.63$, $p_2 = -1.17, -0.71, -0.11$, and $p_3 = 0.035, 0.031, 0.042$ for $N = 2$, 3, and 6, respectively. These values correspond to relatively small corrections to our original formula, but, as seen in Fig. 5, the analytic theory is now very close to the simulation results. Thus we have an analytic theory that describes the first contact time over more than an order magnitude of patch size and for a broad range of well depths.

V. DISCUSSION: GENERALIZATION AND RELEVANCE TO BIOLOGY

A. First-contact time between two particles

Our results, as summarized by Eqs. (23) and (24), can be extended to treat several other cases of physical interest. For example, in two dimensions, Eq. (20) can be used to calculate the first-contact time for a particle in a harmonic potential well moving to another fixed particle, if we regard the fixed particle as a patch. We are justified in using our formula in this case despite the absence of a sharp reflective boundary, since the attractive potential constrains the moving particle much as a reflective boundary would. Because of the exponential decay of the Boltzmann factor with increasing energy, the particle will be very unlikely to have an energy much greater than E_0, so it will move to radii only slightly greater than R. The first-contact time for the particle is the time when the center-to-center distance first becomes smaller than the sum of the particles' radii. Then from Eq. (20) we have

$$W \approx \frac{(R-R_0)^2}{4D}\frac{\pi}{\theta_p}\frac{e^{\beta E_0}}{(\beta E_0)^2}, \quad (25)$$

where R is the distance between the fixed particle and the bottom of the well, R_0 is the sum of the radii of the two particles, and $E_0 = (k/2)(R-R_0)^2$ is the potential energy at contact. The effective patch size should be related to the particle radius, the distance between the two particles, and the spring constant. Larger R_0, and smaller R and k, result in a larger effective patch size. To simplify the calculation, we take the patch size θ_p to be $(R_0/2)/(R-R_0)$, half the angle subtended by the fixed particle. We test Eq. (25) by Brownian dynamics simulations similar to those described above, for E_0 between $4k_BT$ and $11k_BT$, and R_0/R varying from 0.1 to 0.3. The prediction of Eq. (25) is within a factor of 2 of the simulation results over several orders of magnitude variation in W. Use of a more accurate formula to estimate θ_p improves the agreement to about 50%.

On the basis of a similar analysis, we can obtain the first-contact time for two identical moving particles, each of them starting its motion at the center of a harmonic potential well. The distance between the minima of the potential wells is R, both wells have spring constant k, and both particles have diffusion constant D. Our Brownian dynamics simulations of this process show that the particles almost always contact within a very small region (Fig. 6), halfway between the two potential well centers, where the total free energy is minimized. Treating this region as a patch and applying Eq. (25), we find that the first-contact time between two particles in two dimensions is

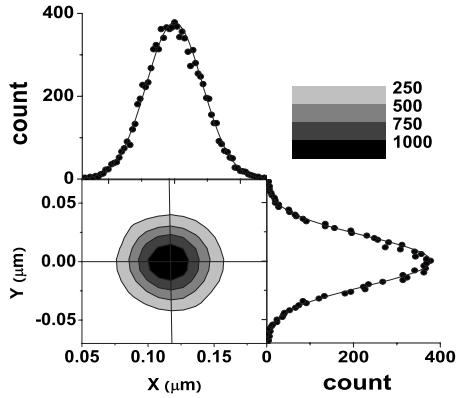

FIG. 6. Contour plot of the distribution of contact position between two particles in two-dimensional space. Each particle is in its own harmonic potential well. Circles represent the simulation results. Lines in the one-dimensional projections are Gaussian distributions fitted to the simulations. Distance between two potential minima is 0.2375 μm. The vertical line is $x=1/2\times0.2375$ μm, halfway between the minima.

$$W \approx \frac{\pi(R-R_0)^3}{4(2D)(2R_0)}\frac{e^{\beta E_0}}{(\beta E_0)^2}, \tag{26}$$

where D is replaced by $2D$, the mutual diffusion constant of the particles, and we have used $\theta_p=R_0/[(R-R_0)/2]$. This differs from our previous formula for θ_p in two ways. First, $R-R_0$ is replaced by $(R-R_0)/2$, which is the distance from the energy minimum to the meeting point. Second, the effective patch size is taken to be twice the patch size for a moving particle to a fixed particle because the fluctuation in the position of the second particle enlarges the target area for the first particle. The potential energy at the average point of contact is

$$E_0 = 2\frac{k}{2}\left(\frac{R-R_0}{2}\right)^2 + 2\frac{k_BT}{2}. \tag{27}$$

The first term on the right side is the energy of the two particles at the mean contact position, which minimizes the total free energy. The additive constant is present because the contact position has a thermal spread. Simulations of the contact between the particles show that the distribution of the contact position is similar to that of a particle in an isotropic harmonic potential well (Fig. 6). The total free energy then has an additional term resulting from the fluctuation of the contact position in this potential well. Since each direction of motion is associated with a fluctuation energy of $k_BT/2$, the correction is simply $Nk_BT/2$, where N is the number of dimensions. Our simulations (data not shown) are close to the calculated results from the above equations. As in the particle to fixed particle case, Eq. (26) is within about a factor of 2 of the simulation results, and improved treatment of R_0 reduces the error to about 50%.

B. First-contact time between two actin filaments

As an illustrative biophysical application of this theory, we calculate the first-contact time between two constrained actin filaments as a function of their separation. In our previous work [17], we used a normal-mode analysis to simulate the bundling of two filaments that had fixed positions and orientations at their bases, but were not able to obtain an analytic theory. This work showed that the motion of a filament with one end fixed and the other end free can be regarded as the sum of the motion of several normal modes, and the motion of each mode coefficient is the same as that of a particle in a harmonic potential well. The frequency of the motion of the normal modes increases rapidly with the order of the mode. Since there is a large separation in the normal-mode frequencies, the motion of each segment of the filament may be thought of as the motion due to the x and y components of the first mode, but with a larger effective radius resulting from the motion of the higher modes. Thus the configuration of each filament is described by two variables, and our two-dimensional analysis applies.

We thus use Eq. (26) for the first-contact time between two particles, to calculate the first-contact time between the filaments, where D is the diffusion coefficient for the motion of each filament tip due to the first mode. The simulations of the filament-contact process show that most of the first contacts occur at the tips of the filaments, and, as in the single-particle case, at a lateral position halfway between the bases of the filaments. We take $R_0=2R^{\text{eff}}$, where R^{eff} is the effective radius of each filament tip,

$$R^{\text{eff}} = R^0 + \sqrt{\sum_{n=2}^{\infty}\langle\alpha_n^2X_n^2(L)\rangle} = R^0 + 0.1L\left(\frac{L}{l_p}\right)^{1/2}, \tag{28}$$

L is the filament length, n is the order of the normal mode, X_n is the eigenfunction, $l_p=10$ μm is the persistence length of the actin filaments, and α_n is a time-varying coefficient. The second equality is straightforwardly derived from the results of Ref. [17]. The square root in Eq. (28) is the rms displacement due to the higher modes. We take $R^0=R^{\text{cutoff}}/2=0.09$ μm, where R^{cutoff} is the cutoff distance of the interaction between two filaments. We consider filaments of length 0.6 μm as a case for comparison with our preceding theory. Using the methods of [17], we obtain $R^{\text{eff}}=0.0235$ μm, so $R^0=0.047$ μm; we also have [17]

$$D = D_{\text{mon}}\frac{aX_1^2(L)}{\int_0^L X_1^2dz} = 4D_{\text{mon}}\frac{a}{L} = 0.72\ \frac{\mu\text{m}^2}{\text{s}},$$

where $D_{\text{mon}}=40$ $\mu\text{m}^2/\text{s}$ is the free actin monomer diffusion constant, and $a=0.0027$ μm is the length per subunit. The spring constant for the motion of the filament tip due to the first normal mode is

$$k = \frac{k_BTl_p\lambda_1}{X_1^2(L)}\int_0^L X_1^2dz = \frac{3.1k_BTl_p}{L^3} = 144\frac{k_BT}{\mu\text{m}^2}, \tag{29}$$

where λ_1 is the first eigenvalue of the beam eigenvalue equation $d^4X_N/dz^4=\lambda_NX_N$ [17]. The first-contact time as a function of separation R for $L=0.6$ μm is then, from Eqs. (26) and (27),

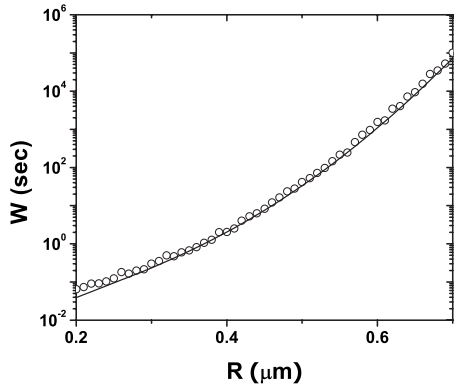

FIG. 7. Simulations (open circles) and calculations (line) of the first-contact time between two actin filaments with length $L=0.6$ μm as a function of distance R between their bases. The two filaments are fixed and parallel at one end, and free at the other.

$$W = \frac{\pi(R-R_0)^3}{16DR_0} \frac{e^{(\beta k/4)(R-R_0)^2+1}}{[(\beta k/4)(R-R_0)^2+1]^2}. \quad (30)$$

Figure 7 shows this formula along with simulations of the first-contact time between two filaments with length 0.6 μm. The theory and simulation are remarkably close over a very large time range, within 50% over most of the range, and within a factor of 2 for small R. The main feature seen in the plot is a strong dependence of W on R, coming from the exponential in Eq. (30). This exponential is an activation-energy term, as expected from conventional rate theories. The $[(\beta k/4)(R-R_0)^2+1]^2$ term is an additional energy barrier dependence not present in most previous approaches. This correction ranges from 3.2 to 260 over the range of separations that we study, and is crucial for obtaining agreement with the simulations. The $1/R_0$ term reflects the extra time that it takes for thin filaments to find each other. We also note that Eq. (30) predicts a very rapid dependence of W on L [via k, see Eq. (29)], as was observed in our earlier work [17].

C. Summary and outlook

The preceding sections have used simulation and analytic theory to calculate the first-contact time of a particle to a patch on a spherical boundary. Our main conclusions are the following: (1) for weak potentials, the first-contact time increases with decreasing patch size, but less rapidly than the inverse of the patch area; (2) for strong potentials, the first-contact time is inversely proportional to the patch area; (3) the crossover between these regimes occurs at an energy inversely proportional to the patch radius; and (4) first-contact time problems involving particles or more extended objects such as biopolymers can be accurately mapped onto our particle-to-a-patch problem. Other phenomena, such as folding and aggregation of proteins, may also be treated by our multidimensional formalism. Most protein folding models treat the process as a one-dimensional transition between two stable states separated by an energy barrier. However, if there is more than one relevant reaction coordinate, and folding corresponds to a specific combination of the reaction coordinates, a treatment based on the present analysis might be more appropriate. Similarly, the problem of protein aggregation may involve multiple internal degrees of freedom for the proteins, again requiring a multidimensional analysis. These and other potential applications may be treatable by minor modifications to the present formalism.

ACKNOWLEDGMENTS

We appreciate a careful reading of this paper by Frank Brooks. This work was supported by the National Science Foundation under Grant No. DMS-0240770 and the National Institutes of Health under Grant No. R01-GM067246.

[1] P. Hänggi, P. Talkner, and M. Borkovec, Rev. Mod. Phys. **62**, 251 (1990).
[2] E. Pollak and P. Talkner, Chaos **15**, 026116 (2005).
[3] E. P. Wigner, Z. Phys. Chem. Abt. B **19**, 203 (1932).
[4] H. Eyring, J. Chem. Phys. **3**, 107 (1935).
[5] R. A. Marcus, J. Chem. Phys. **20**, 359 (1952).
[6] O. Klein, Ark. Mat., Astron. Fys. **16**, 1 (1922).
[7] H. A. Kramers, Physica (Amsterdam) **7**, 284 (1940).
[8] F. A. Lindemann, Trans. Faraday Soc. **17**, 598 (1922).
[9] C. N. Hinshelwood, *The Kinetics of Chemical Change in Gaseous Systems* (Clarendon, Oxford, 1929).
[10] C. N. Hinshelwood, Proc. R. Soc. London, Ser. A **113**, 230 (1926).
[11] E. Schrödinger, Phys. Z. **16**, 289 (1915).
[12] B. Widom, J. Chem. Phys. **30**, 238 (1959).
[13] J. Zhu and A. E. Carlsson, Eur. Phys. J. E **21**, 209 (2006).
[14] H. C. Berg, *Random Walks in Biology* (Princeton University Press, Princeton, NJ, 1983).
[15] H. C. Berg and E. M. Purcell, Biophys. J. **20**, 193 (1977).
[16] O. G. Berg and P. H. von Hippel, Annu. Rev. Biophys. Biophys. Chem. **14**, 131 (1985).
[17] L. Yang, D. Sept, and A. E. Carlsson, Biophys. J. **90**, 4295 (2006).
[18] M. Doi and S. F. Edwards, *The Theory of Polymer Dynamics* (Oxford University Press, New York, 1986).
[19] A. Rich, N. Davidson, and L. Pauling, *Structural Chemistry and Molecular Biology* (W. H. Freeman, San Francisco, 1968).
[20] *Handbook of Mathematical Functions With Formulas, Graphs, and Mathematical Tables*, edited by M. Abramowitz and I. A. Stegun (Wiley, New York, 1972).